Clays and Clay Minerals, Vol. 42, No. 1, 53–62, 1994.

ACIDIFIED OXALATE AND DITHIONITE SOLUBILITY AND COLOR OF SYNTHETIC, PARTIALLY OXIDIZED AL-MAGNETITES AND THEIR THERMAL OXIDATION PRODUCTS

D. C. GOLDEN,[1] D. W. MING,[1] L. H. BOWEN,[2] R. V. MORRIS,[1] AND H. V. LAUER JR.[3]

[1] NASA–Johnson Space Center, Houston, Texas 77058

[2] Department of Chemistry, North Carolina State University, Raleigh, North Carolina 27695

[3] Lockheed ESC, Houston, Texas 77058

Abstract—Submicron-sized (~3–60 nm) powders of Al-substituted magnetite were synthesized in the laboratory by precipitation methods by mixing appropriate molar volumes $FeCl_2$, $FeCl_3$ and $AlCl_3$ solutions and precipitating with 20% NH_4OH. Precipitates were dialyzed for 48 hr to remove excess salts and then freeze-dried. The nominal Al mole fractions [Al_s = Al/(Al + Fe)] in the initial precipitate ranged from 0.001 to 0.42. Portions of the resulting powders were heated sequentially in air at 400° and 500°C. Powders were examined using X-ray diffraction (XRD), transmission electron microscopy (TEM), and visible and near-IR reflectance spectroscopy. Solubilities were determined in ammonium oxalate (pH = 3) and dithionite-citrate-bicarbonate (DCB) solutions. As determined by XRD, the mineralogy of precipitated powder samples was predominantly magnetite. Powders having $Al_s > 0.20$ contained minor goethite and a poorly crystalline iron oxide phase (ferrihydrite?), and powders having $Al_s > 0.25$ also contained gibbsite. The color of the magnetites was black throughout the range of Al-substitution. Powders heated to 400°C were reddish brown; Munsell colors ranged from 5R 2/2 to 10R 3/4 for Al_s from 0.1–41.5%, respectively. By XRD, these powders were maghemite, but hematite was also detected by Mössbauer spectroscopy. XRD and Mössbauer data indicate powders heated to 500°C are hematite; their Munsell colors are not noticeably different from the corresponding 400°C samples. Mean crystallite dimensions (MCDs) of the magnetite powders increase with the Al mole fraction from ~10 nm for Al_s = 0.001% to a maximum value of 35 nm for $Al_s = 0.15$ and decrease slightly with further increasing Al substitution. Heating magnetite powders to 400°C did not change the MCDs significantly. Heating to 500°C resulted in hematites having MCDs larger than those for corresponding precursor magnetites for $Al_s < 0.10$. The opposite is true for hematites derived from magnetites having $Al_s > 0.10$. For hematite powders with $Al_s > 0.05$, MCD decreased with increasing Al-substitution. Solubilities of powders in oxalate solutions were independent of Al content and decreased in the order unheated samples (mostly magnetite) >400°C-heated samples (maghemite + hematite) >500°C-heated samples (hematite). All powders dissolved completely in DCB. The low crystallinity of the magnetite powders and the presence of ferrous iron are responsible for their relatively high solubility in oxalate solutions.

Key Words—Aluminum substitution, Electron microscopy, Hematite, Maghemite, Magnetite, Oxidation, Solubility.

INTRODUCTION

Iron oxides in soils can be selectively removed by taking advantage of their differential solubility to various reagents. Traditionally, the most popular procedure is to selectively remove "amorphous or poorly crystalline" iron oxides and then remove "crystalline" iron oxides (McKeague and Day, 1966; Schwertmann, 1964; Saunders, 1965). Acidified ammonium oxalate (pH = 3) is used for dissolving amorphous or poorly crystalline iron oxides. Dithionite-citrate-bicarbonate (DCB) is used for extraction of all forms of iron oxides that are not protected (i.e., "free") by an insoluble barrier such as a silica concretion surrounding oxide particles. The ratio Fe_o/Fe_d is used to measure poorly crystalline iron oxides as a fraction of the total Fe-oxides and is often used as an index for soil profile development (McKeague and Day, 1966). Unfortunately, some well-crystalline, ferrous-containing iron oxides (e.g., magnetite) are soluble in oxalate (Pawluk, 1972) and would be considered poorly crystalline by the above criteria.

Stoichiometric magnetite has a formula Fe_3O_4 and a ferrous to ferric ratio of 0.5. In natural systems, magnetite is often cation-deficient (ferrous to ferric ratio lower than 0.5) and contains other elements (e.g., Al, Zn, Cu, Mn, Ni, Co, Mg, Cr, and Ti: Anand and Gilkes, 1984). The substitution of cations in the magnetite structure and the changes in oxidation state of iron may influence its solubility with respect to oxalate and DCB solutions. For example, does Al substitution affect the oxalate solubility of magnetite or its oxidation products maghemite (γ-Fe_2O_3) and hematite (α-Fe_2O_3)? The objectives of the present work were to study the effect of Al substitution on the oxalate and DCB solubility of synthetic, Al-substituted magnetites and their thermal oxidation products. X-ray diffraction (XRD), Mössbauer, visible and near-IR diffuse reflectance spectroscopy, and color data were also obtained.

Table 1. Total iron, ferrous iron, and aluminum concentrations [Fe_t, $(Fe^{2+})_t$, and Al_t], mole fraction $Al_s = Al/(Al + Fe)$, oxalate (o) and DCB (d) extractable Fe and Al, Fe_o/Fe_d ratio, and mineralogy of powders synthesized at room temperature.

Sample	Fe (wt. %)	$(Fe^{2+})_t$ (wt. %)	Al_t (wt. %)	Al_s (mole fr.)	Fe_d (wt. %)	Al_d (wt. %)	Fe_o (wt.%)	Al_o (wt. %)	Fe_o/Fe_d	Al_o/Al_d	Mineralogy[1] (by XRD)
MT-RT-00	67.1	1.9[2]	0.05	0.001	65.4	0.00	66.6	0.11	1.02	—	mt
MT-RT-05	61.1	4.1	1.69	0.054	61.6	1.59	63.7	1.73	1.03	1.09	mt
MT-RT-10	57.9	4.0	3.15	0.101	56.6	3.17	58.4	3.02	1.03	0.95	mt
MT-RT-15	53.6	4.6	4.66	0.152	52.3	4.66	52.6	4.23	1.01	0.91	mt
MT-RT-20	50.2	2.9	6.08	0.200	46.9	6.01	46.4	5.13	0.99	0.85	mt
MT-RT-25	46.1	1.3	7.45	0.251	43.0	7.31	31.3	4.81	0.73	0.66	mt + gt
MT-RT-30	40.7	0.6	8.56	0.303	40.0	8.55	27.1	4.91	0.68	0.57	mt + gt + gb
MT-RT-35	40.5	1.4	10.94	0.358	38.1	7.79	20.9	4.65	0.55	0.60	mt + gt + gb
MT-RT-40	36.7	1.4	12.57	0.415	35.7	7.33	14.8	4.45	0.42	0.60	mt + gt + gb

[1] mt = magnetite, gt = goethite, gb = gibbsite.
[2] Stoichiometric magnetite (Fe_3O_4) has 24.1 wt. % Fe^{2+}.

MATERIALS AND METHODS

Magnetite synthesis and oxidation

Magnetite was synthesized by mixing solutions of ferrous and ferric chlorides in the mole ratio 2:1 and then adding 20% ammonia solution to a final pH of 12. The precipitate was aged for 24 hr and then dialyzed against deionized water (~48 hr) until no more chloride was detected in the dialyzate. The dialyzed product was quick-frozen in liquid nitrogen and freeze-dried. Al substitution was obtained by replacing a fraction of $FeCl_3$ in the initial solution with the appropriate amount of $AlCl_3$. Nine samples of Al-substituted magnetites were prepared from mixed solutions of $FeCl_3$ and $AlCl_3$ having mole fraction of Al/(Al + Fe) (denote as Al_s) ranging from 0 to 0.4 in steps of 0.05. The resulting powders (MT-RT-00 through MT-RT-40) were heated sequentially in air in a muffle furnace at 400°C for 4 hr (MT-400-00 through MT-400-40) and then at 500°C for 6 hr (MT-500-00 through MT-500-40).

Analytical methods

Total chemical analysis (TCA) and ferrous iron determination. Powder samples were dissolved by digesting 100 mg of sample with 5 ml of HF and 1 ml of 10% 1,10-phenanthroline in ethanol (Stucki, 1981). The digest was diluted to 100 ml with water and absorbance read at 510 nm for ferrous iron determination. The whole procedure was performed in the dark under a safe light. Standards were made from ferrous ammonium sulfate and treated in similar fashion to the samples. Total Fe and Al were determined by atomic absorption spectroscopy. An air-acetylene flame was used for Fe and a nitrous oxide-acetylene flame for Al.

Acidified ammonium oxalate (pH = 3) extraction (oxalate extraction). Solutions of 0.3 M ammonium oxalate and 0.3 M oxalic acid were mixed to make a pH = 3 solution of oxalate (Schwertmann, 1964; McKeague and Day, 1966). Approximately 20 mg samples were weighed into 40 ml polypropylene tubes and 20 ml of oxalate solution was added. The tubes were capped, covered with Al-foil to prevent any exposure to light, and shaken in a horizontal shaker for 4 hr. After shaking, suspensions were centrifuged and supernatants were collected for analysis of Fe and Al.

Dithionite-citrate-bicarbonate (DCB) extraction. Citrate-bicarbonate buffer (pH = 7.3) was prepared as described by Jackson (1974). Samples weighing ~40 mg were placed in 50 ml polypropylene centrifuge tubes. Citrate-bicarbonate buffer was added to the tube to make a solid to solution ratio of 1 to 1000, and the mixture was placed in an 80°C water bath. After the tube had reached a temperature of 80°C, approximately 1 g of sodium dithionite was added to the sample mixture. The tube was maintained at 75°–80°C and occasionally stirred. When the reaction ceased, the contents were centrifuged. The decantate was analyzed for Fe and Al using atomic absorption spectroscopy. Care was taken for the temperature to not to exceed 80°C during the procedure.

X-ray diffraction (XRD). Powders were mounted in cavities carved on glass slides and X-rayed with CuKα radiation using a Scintag XDS 2000 X-ray diffractometer configured with a graphite monochromator, a 0.3 mm receiving slit, and a 0.5 mm divergence slit. Kα_2 radiation stripping was done by a software routine. XRD line broadening was used to measure the mean crystallite dimensions (MCDs) of magnetite and hematite particles using Scherrer equation. The line corresponding to 0.269 nm (d104) peak was used for hematite, and that for 0.253 nm (d110) peak was used for magnetite. Corrections for instrumental broadening were carried out using a quartz powder pattern obtained using the same instrument settings (Zussman, 1977).

Electron microscopy. For transmission electron microscopy (TEM), the oxides were dispersed in distilled water, and a drop of the suspension was evaporated on a holey carbon film. The dried sample was carbon-coated prior to examination with a JEOL 2000 FX scanning transmission electron microscope (STEM).

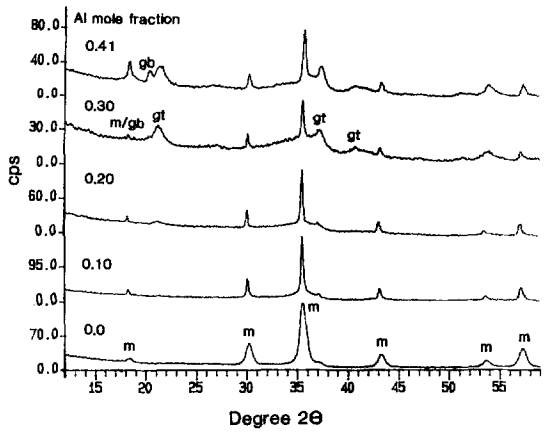

Figure 1. X-ray diffraction (XRD) patterns for selected magnetite samples (0.1, 10.1, 20.0, 30.3, 41.5 mole % Al). Note the appearance of goethite peaks (0.416 and 0.245 nm) and gibbsite peaks (0.485 and 0.437 nm) above 30.3 mole % Al. Note the line broadening in the 0.1 mole % Al sample due to small particle size.

Mössbauer and reflectance spectroscopy. Mössbauer spectra were obtained at room and liquid nitrogen temperatures only for the unheated Al-magnetites using a 25 mCi ^{57}Co/Rh source at room temperature. Velocity calibrations were done by laser interferometry. Visible and near-IR reflectance spectra were obtained at 293 K on a Cary-14 spectrophotometer configured with a 9-inch diameter integrating sphere. The spectra were obtained relative to a Halon standard and converted to absolute reflectivity (Weidner and Hsia, 1981). The color of the powder samples was determined using Munsell color charts.

RESULTS

Total chemical analysis and XRD

Values of Al_s in the precipitates, which were calculated from total dissolution data, are similar to those

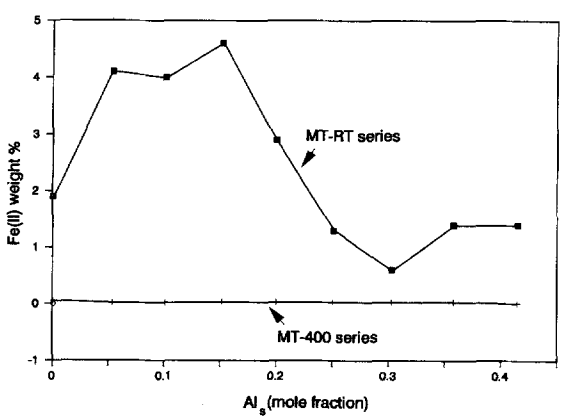

Figure 2. Weight percent Fe^{2+} in magnetite and 400°C heated magnetite samples determined colorimetrically for samples of Al_s 0.001 to 0.41.

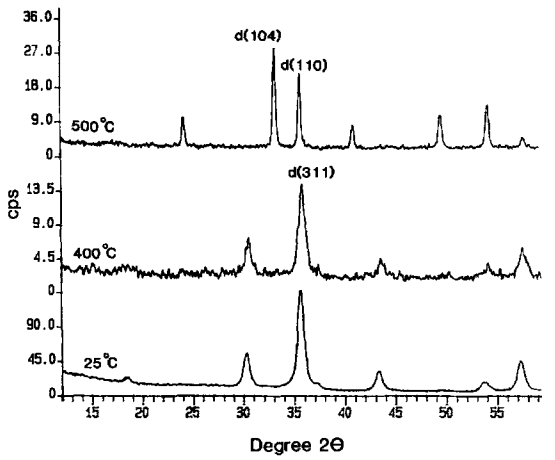

Figure 3. XRD patterns for 0 mole % Al magnetite at 25°C, after heating for 4 hr at 400°C (maghemite), and after heating for 6 hr at 500°C (hematite).

of the reactant mixture (Table 1). Observed values of Al_s represent the degree of Al substitution in magnetite only if no other Al-bearing phases are present. XRD data (Figure 1; Table 1) indicate magnetite as the major phase present for samples MT-RT-00 through MT-RT-20. Both magnetite and goethite (0.418 nm peak) were detected in sample MT-RT-25. Magnetite, goethite, and gibbsite (0.46 nm peak) were detected in samples MT-RT-30 through MT-RT-40. Additional minerals in minor quantities (e.g., <5 wt. %) or poorly crystalline (X-ray amorphous) minerals (e.g., ferrihydrite) are not easily detected by XRD specially in the presence of more crystalline phases. Broad humps in the XRD background near 0.25, 0.22 (Figure 1), and 0.15 nm (not shown) suggested possible presence of ferrihydrite, the amount of which appears to increase with increase in Al_s. Presence of ferrihydrite is also supported by Mössbauer and TEM data discussed later.

The magnetites have a maximum Fe^{2+} content of ~4.5 wt. %, which is considerably lower than the value of 24.1 wt. % for stoichiometric magnetite. The magnetites are, therefore, strongly cation deficient (partially oxidized). This is apparently the general case for magnetite prepared by wet chemical methods (Schwertmann and Murad, 1990; Sidhu *et al.*, 1981). Upon heating the magnetite powders to 400°C for 4 hr in the air, the Fe^{2+} was completely oxidized to Fe^{3+} (Figure 2). Magnetite-like XRD patterns and near-zero ferrous Fe content indicates these powders are maghemite. However, Mössbauer spectra of these samples indicated the presence of some hematite in addition to maghemite. Hematite was the only phase detected by XRD and Mössbauer data when the samples in the MT-400 series were heated to 500°C for 6 hr. XRD data for the powder MT-RT-00 with $Al_s = 0.001$ along with those of its heated products is shown in Figure 3.

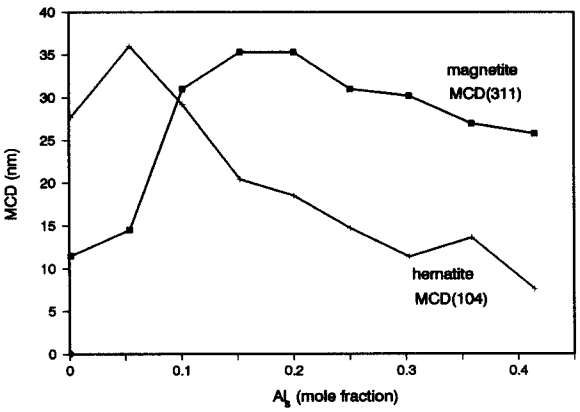

Figure 4. Mean crystallite dimensions of magnetite and hematite produced by heating magnetites for samples of Al_s 0.001 to 0.41.

Goethite content increased with increase in Al_s for the MT-RT series in agreement with a similar effect reported by Schwertmann and Murad (1990).

Mean crystallite dimensions (MCDs) for magnetite (unheated powders) and hematite (500°C powders) were calculated using the Scherrer equation (Zussmann, 1977). The MCD in a direction perpendicular to the [311] crystallographic plane for magnetite has an initial sharp increase with Al content up to $Al_s \approx 0.15$ and then decreases slowly with further Al substitution (Figure 4). Hematite MCDs (perpendicular to [104] plane) also increases initially with Al content up to $Al_s = 0.054$ and then decreases in MCD with further increases of Al (Figure 4). Magnetite samples MT-RT-00 (Al_s = 0.001) and MT-RT-05 (Al_s = 0.054) have MCDs less than 20 nm; all other MCDs are ~30 nm. The MCD calculations were done assuming that no strain was present in the crystallites. Strain, if present, may also cause XRD line broadening.

Transmission electron microscopy (TEM)

TEM photomicrographs (Figures 5a–5d) and selected area electron diffraction patterns (SAED) of magnetite, maghemite, and hematite particles (Figures 5e–5g) are shown for unsubstituted (Al_s = 0.001) samples. The dimensions of magnetite particles in MT-RT-00 are 3–15 nm across. The MCD(311) estimated from line broadening is on the same order (~12 nm). As Al_s increases from 0 to 0.2, the magnetite particle size increases as seen by TEM (Figure 5j) and XRD measured values of MCD(311) also increase (Figure 4). From Al_s 0.2 to 0.4, a slight decrease in MCD is observed. The MCD(311) of 35 nm for MT-RT-20 is within the 5–60 nm range observed by TEM. Electron diffraction patterns of both MT-RT and MT-400 series samples show superlattice reflections indicating the ordering of vacancies. Formation of hematite (MT-500 series) has caused considerable solid phase alteration, as suggested by the rounded edges (Figure 5d) and the well-formed structure (Figure 5h). Hematite has the best ordering of atoms in single domain particles.

The Al_s = 0.20 magnetite sample (MT-RT-20), however, suggests heterogeneity in composition (Figure 5i). The rounded particles coated with finer particles are magnetite and the elongated needle-like ones are goethite or lepidocrocite. The very fine particles (<5 nm) may be a ferrihydrite-like phase, as suggested by the two-line electron diffraction pattern (Figure 5k, 0.25 nm and 0.15 nm). There were occasional large particles of magnetite that yielded spot patterns (not shown). A ring pattern was also noted for fine hematite particles formed from ferrihydrite-like phase and a spot pattern for the large particles of hematite formed by heating the Al_s = 0.20 magnetite powder (Figure 5l). In samples with higher Al contents, an occasional lepidocrocite crystal was also detected (presence of 0.6 nm lattice fringes).

Oxalate and dithionite-citrate-bicarbonate (DCB) extractions

Our magnetite samples are essentially completely soluble in oxalate. The samples heated to 400°C (maghemite + hematite) are partially soluble. Samples heated to 500°C (hematite) are the least soluble of the three sets of samples considered (Figure 6). Within each sample set, oxalate-soluble Fe deviates from total Fe as Al_s increases (Table 1). This probably results from the presence of the oxalate-insoluble minerals goethite and gibbsite at high Al contents (Figure 1). Ferrihydrite, if present, would completely dissolve in oxalate (Schwertmann, 1964).

DCB extractions were done only for magnetite (unheated) and hematite (500°C) samples. Concentrations of DCB-extractable Fe are similar to total Fe concentrations for unheated samples (Table 1), indicating that all oxides containing Fe (e.g., magnetite, goethite, and ferrihydrite) dissolved in DCB. The deviation of Al_t from Al_d for two samples with the highest Al content (MT-RT-35 and -40) is consistent with the formation of gibbsite as observed in XRD data. The results for samples heated to 500°C are similar.

Mössbauer spectroscopy of Al-magnetites

Mössbauer data for Al-magnetite samples MT-RT-00, MT-RT-05, MT-RT-10, MT-RT-15, and MT-RT-20 (Al_s = 0.001, 0.054, 0.101, 0.152, and 0.20, respectively) are given in Table 2 and Figure 7. Room temperature spectra are characterized by a Fe^{3+} doublet, whose percentage area increases markedly from only 1% for MT-RT-00 to 73% for MT-RT-20, and one or two magnetic sextets. The two-sextet spectra are consistent with magnetite where sextets #1 and #2 result from tetrahedral (occupied by Fe^{3+}) and octahedral (occupied by Fe^{2+} and Fe^{3+}) sites, respectively. The single, very broad, and asymmetric sextet for the unsubstituted sample (MT-RT-00) results from an un-

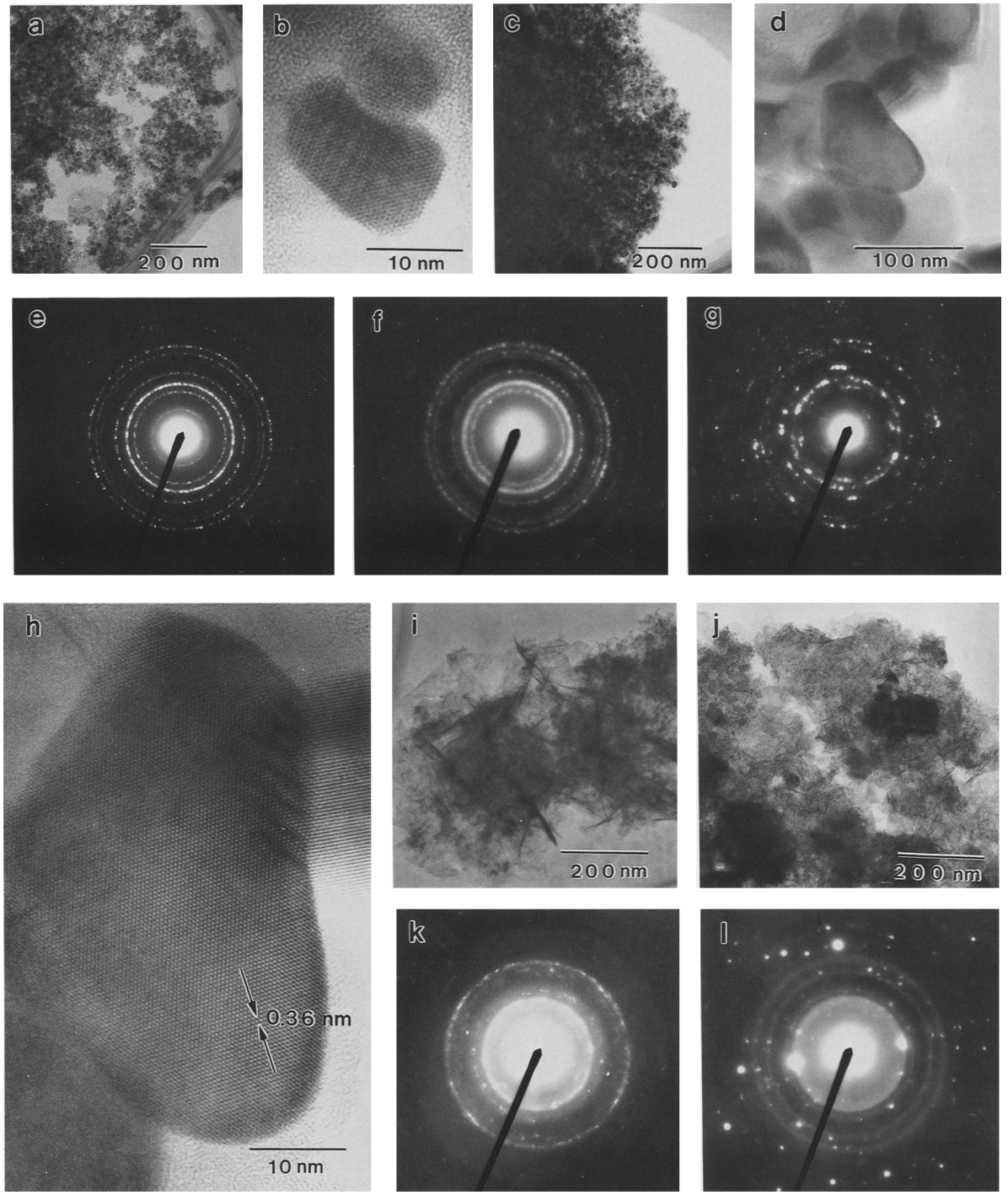

Figure 5. Transmission electron micrographs (TEM) of Al-magnetite and its heat transformation products: a) TEM of 0.1 mole % Al magnetite; b) high resolution TEM of two magnetite particles of 0.1 mole % Al; c) maghemite produced by heating magnetite in (a) to 400°C for 4 hr; d) hematite produced by heating maghemite in (c) to 500°C for 6 hr; e) selective area electron diffraction pattern (SAED) of (a); f) SAED pattern of (c); g) SAED pattern of (d); h) high-resolution TEM image of hematite particle from (d), beam direction is along the ⟨100⟩ zone axis and the 0.36 nm corresponds to spacing d(012); i) TEM of 20 mole % Al product; j) hematite produced from 20 mole % Al product, (K) SAED pattern for (i), and SAED pattern for (j).

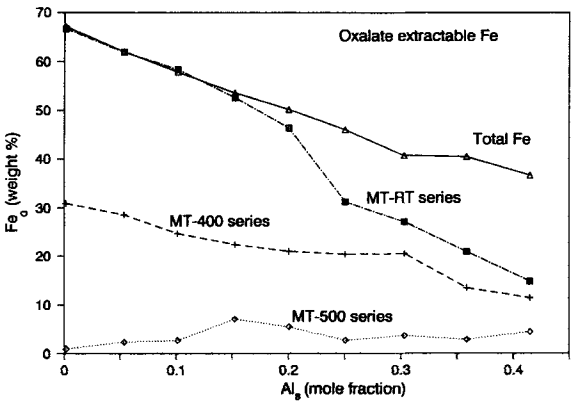

Figure 6. Total and acidified ammonium oxalate (oxalate) soluble Fe (wt. %) in magnetite, maghemite, and hematite of 0.001 to 0.41 Al_s oxide samples.

resolved superposition of the two sextets. This condition implies that the ratio of ferric to ferrous iron in the octahedral site is high so that the Mössbauer parameters of the two sites are nearly the same. This is consistent with the low concentration of Fe^{2+}, which is ~2 wt. % as compared with 24 wt. % for stoichiometric magnetite. For the other four samples, the chemically-determined Fe^{2+} concentration is much larger and two clearly-resolved sextets are present in the Mössbauer spectra; one corresponds to mixed valence Fe^{2+}–Fe^{3+} in octahedral sites and the other to Fe^{3+} in tetrahedral (and possibly octahedral) sites. In addition, there is an increasing proportion of the Fe^{3+} doublet with increasing Al substitution. This doublet may correspond to a separate phase, and increasing proportion of the ferric doublet with increasing Al_s together imply that the ratio of ferric to ferrous iron in the tetrahedral site is lower relative to MT-RT-00 and also decreases as Al_s increases. It is not known how Al is partitioned between the doublet phase and magnetite or how it is partitioned between tetrahedral and octahedral sites of magnetite. In a recent study (Schwertmann and Murad, 1990), no preferential affinity of Al for the magnetite sites was observed.

An appreciable fraction of the RT doublet remains at 77 K for samples with Al_s = 0.152 and 0.20. Because ferrihydrite is still a doublet at 77 K (Murad *et al.*, 1988), this may be evidence for a ferrihydrite-like phase, which would be X-ray amorphous and could be Al-substituted. Jolivet *et al.* (1992) also found a similar doublet in unsubstituted magnetites prepared in a similar fashion, but only for low Fe^{2+} concentration in the solution. The doublet disappears completely at 77 K for samples with Al_s = 0.001 and 0.054 and shows relaxation broadening for the 0.101 Al_s. For these samples the room temperature doublet can be assigned to small particles of ferric oxide which become magnetically ordered at 77 K or higher.

The octahedral mixed valence sextet #2 persists at 77 K with no reduction in intensity for samples with 0.152 and 0.20 Al_s. This is quite different from pure magnetite, which undergoes the Vervey transition at about 120K, below which the Fe^{2+} and Fe^{3+} become distinct. If the magnetite is partially oxidized (cation deficient), however, the transition temperature is lowered and no longer sharp (Haley *et al.*, 1989). The two

Table 2. Mössbauer parameters IS (isomer shift), quadrupole splittings (QS), hyperfine field (B_{hf}) and relative spectral area (RA) at room temperature and 77 K for the powders synthesized at room temperature. Quadrupole splitting of sextets was constrained to zero during the fitting procedures. IS is relative to metallic iron at room temperature.

			Sextet #1 (tet.)			Sextet #2 (oct.)			Fe^{3+} Doublet		
Sample	T (K)	Al_s (mole fr.)	IS (mm/s)	B_{hf} (T)	RA (%)	IS (mm/s)	B_{hf} (T)	RA (%)	IS (mm/s)	QS (mm/s)	RA (%)
MT-RT-00	RT	0.001	0.34	46.4	99	nd[1]	nd	nd	0.35	0.59	1
	77		0.28	50.9	46	0.54	51.4	54	nd	nd	nd
MT-RT-05	RT[2]	0.054	0.32	48.1	80	0.59	45.1	10	0.30	0.68	10
	77		0.45	50.8	72	0.48	46.1	28	nd	nd	nd
MT-RT-10	RT	0.101	0.31	48.4	28	0.60	45.2	31	0.33	0.69	42
	77		0.45	51.1	32	0.69	46.5	15	0.41	—[3]	52
MT-RT-15	RT	0.152	0.31	48.6	22	0.62	45.2	21	0.33	0.68	57
	77		0.43	51.0	35	0.85	47.1	27	0.45	0.80	38
MT-RT-20	RT	0.200	0.31	48.4	13	0.61	45.0	13	0.32	0.68	73
	77		0.44	50.9	25	0.91	46.7	13	0.44	0.74	63
Magnetite[4]	RT	0	0.26	48.6	—	0.70	46.2	—			
Maghemite[4]	RT	0	0.32	49.9	—						

[1] nd = not determined.
[2] Spectra fitted to a distribution of hyperfine fields; field of maximum probability is reported.
[3] Broad relaxation peak with no clearly defined splitting.
[4] From Morris *et al.* (1985). Single-sextet fit for maghemite.

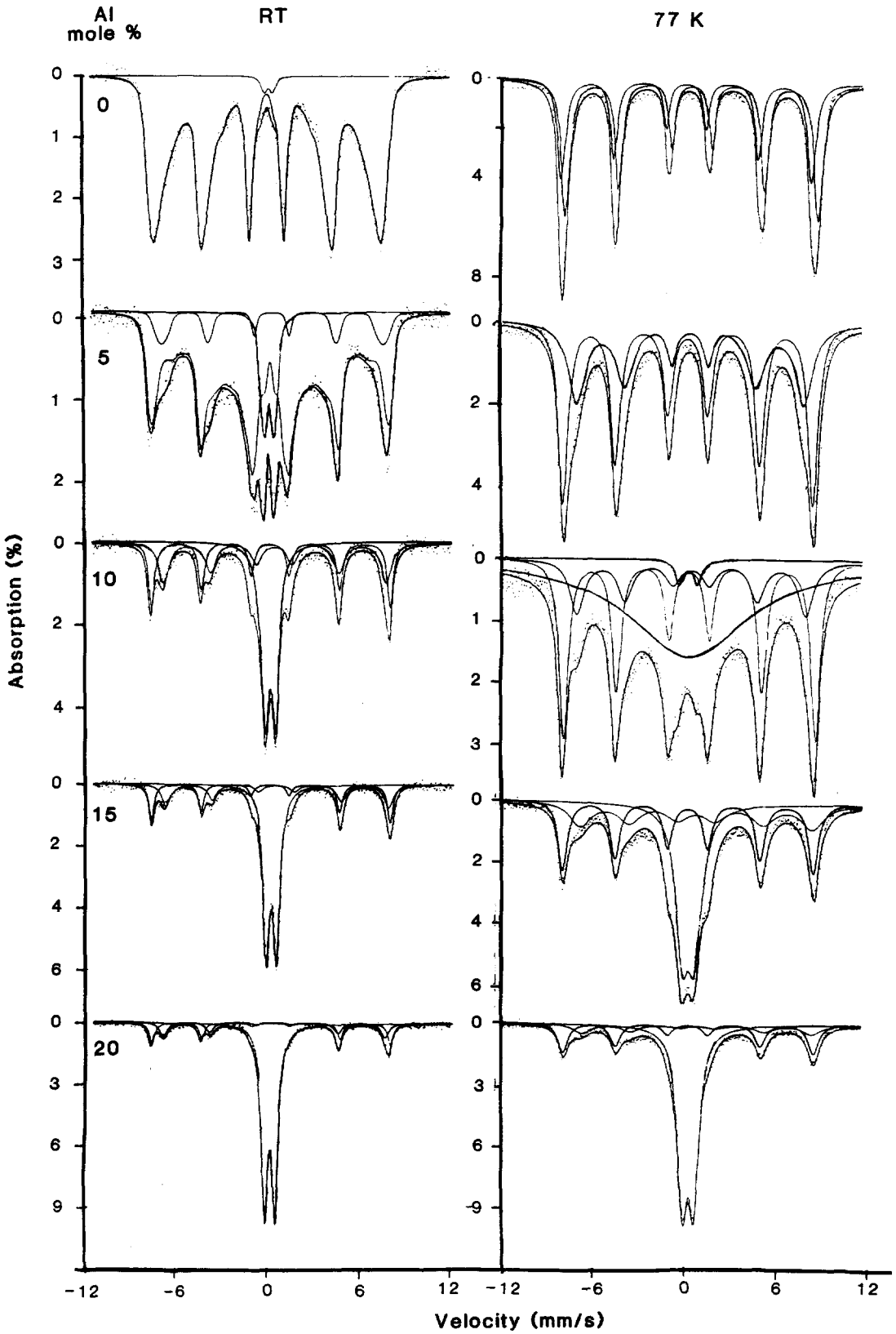

Figure 7. Mössbauer spectra at room temperature and 77 K for five powders from the MT-RT series.

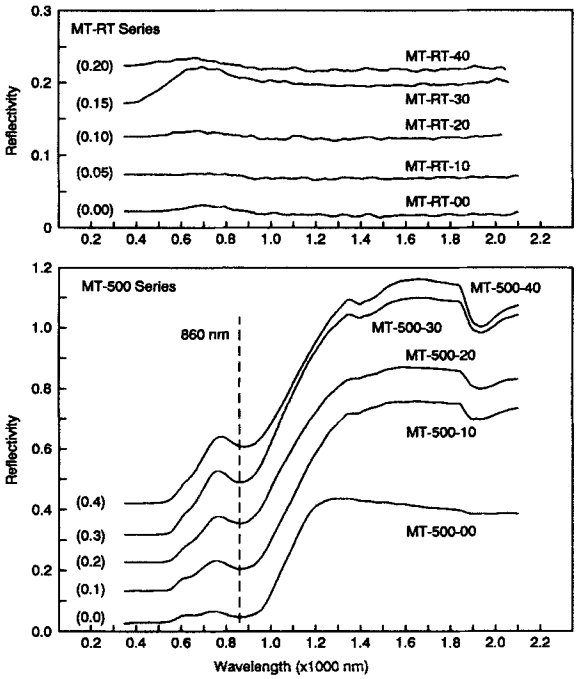

Figure 8. Diffuse reflectance spectra (350–2100 nm) for unheated samples (MT-RT series) and samples heated to 500°C (MT-500 series). Spectra offsets are shown in parenthesis.

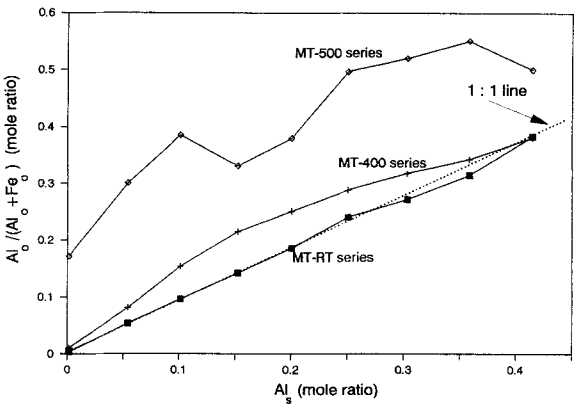

Figure 9. Mole fraction Al in the oxalate (Al_o) extract *vs.* total mole fraction Al in the solid phase (Al_s) for MT-RT, MT-400, and MT-500 series samples. High Al mole ratio in hematite extract probably indicate surface migration of Al during heating.

samples with highest Al show this latter effect. Samples 0.001 and 0.054 Al_s show no sextet #2 for the mixed valence Fe at 77 K, while the proportion is decreased for 0.102 Al_s sample (and partially masked by the relaxation effect). The sextet #2 (octahedral) for the 0.001 and 0.054 Al_s samples at 77 K is Fe^{3+} as these samples are highly oxidized (note the low value of IS compared with 0.152 and 0.20 Al_s), and the 0 mole % Al sample has the two overlapping sextets characteristic of maghemite rather than magnetite (consistent with its greater oxidation). Jolivet *et al.* (1992) in preparing magnetite in a similar fashion to what we have done, observed the formation of two types of particles, some smaller (~4 nm) and others larger (>25 nm). The greater the oxidation of Fe^{2+}, the more of the smaller variety formed. The extent of oxidation in our samples is within the range of their study.

Reflectance spectroscopy

The reflectance spectra for the cation deficient magnetite samples (Figure 8a) resemble those reported by Morris *et al.* (1985) in that they are all strong absorbers in the 200 to 2000 nm wavelength region and have a broad relative reflectance maximum in the 730–800 nm region. The maximum reflectivity observed (~0.08) is for sample MT-RT-30 which has the lowest Fe^{2+} content. The maximum reflectivity for the remaining MT-RT samples is ~0.04. The reflectance spectra of MT-RT samples heated at 500°C are shown in Figure 8b. The spectrum of MT-500-00 is typical of that for hematite powders (e.g., Morris *et al.*, 1985; Sherman *et al.*, 1985). The band minimum near 860 nm and feature centered near 630 nm result from the ferric $^6A_1 \rightarrow {}^4T_{1g}$ and $^6A_1 \rightarrow {}^4T_{2g}$ electronic transitions, respectively. The edge near 520 nm results from the $2(^6A_1) \rightarrow 2(^4T_{1g})$ pair transition (Sherman and Waite, 1985). The position of the $^6A_1 \rightarrow {}^4T_{1g}$ band shifts from 860 nm to longer wavelengths with increasing Al_s, as observed by Morris *et al.* (1992) for Al-hematites. Reflectance spectra of samples heated to 400°C were similar, indicating the optical dominance of the hematite observed in Mössbauer data.

Bands near 1400 and 1900 nm, which are combination and overtone bands of H_2O and OH fundamentals, are also present in the hematite spectra. Possibilities for their origin include 1) adsorbed water on these fine powders, 2) incomplete dehydroxylation, gibbsite ($Al(OH)_3$) impurities, and 3) retention of hydroxyl or H_2O in the structure of the hematite. In a recent study, Stanjek and Schwertmann (1992) reported the inclusion of hydroxyls in aluminous hematite, where the amount of nonsurface water increased with increase in Al substitution.

DISCUSSION

MT-RT series samples

The ratio of oxalate to DCB extractable Fe (Fe_o/Fe_d) is generally considered as an index for soil development. The ratio $Fe_o/Fe_d = 0$ represents a mature soil, and $Fe_o/Fe_d = 1$ represents an immature soil. As shown in this and other studies (Rhoton *et al.*, 1981; Jolivet *et al.*, 1992), magnetites prepared by precipitation from aqueous solutions (MT-RT samples) have small particle sizes and are strongly cation deficient (partially oxidized). Despite relatively low Fe^{2+} contents (<5 wt. %), all magnetite powders are strong absorbers (black)

at visible and near-IR wavelengths (350–2100 nm). In agreement with Rhoton *et al.* (1981), we found $Fe_o/Fe_d = 1.0$ for $Al_s < 0.20$, which implies that the presence of magnetite can compromise the use of the Fe_o/Fe_d as an index of soil development. For $Al_s > 0.20$, Fe_o/Fe_d decreases with increasing Al_s, which could indicate a decrease in poorly crystalline components with increase in Al substitution. However, the XRD data indicate the difference more likely results from iron-bearing and oxalate-insoluble phases like goethite and gibbsite (Table 1). As shown in Figure 9, the mole fraction of oxalate-extractable Al ($Al_o/(Al_o + Fe_o)$) is linear with a slope of approximately unity for the MT-RT samples, which means that Al and Fe are extracted congruently by oxalate.

Incorporation of Al into the magnetite structure results in maxima in mean crystalline dimension (Figure 4) and Fe^{2+} content (Figure 2) at $Al_s \approx 0.15$. Similar effects have been reported previously (Schwertmann and Murad, 1990) and attributed to stabilization of the magnetite structure by Al substitution. Particle size, Al content, and Fe^{2+} content are related in a complex way because, for unsubstituted magnetites, larger particle sizes are associated with higher Fe^{2+} contents (Jolivet *et al.*, 1992).

Although the magnetites synthesized for this study are completely soluble in both oxalate and DCB, coarse crystals of primary magnetites found in nature are not so readily soluble by either reagent (Jackson, 1974). The difference probably relates to kinetic factors because synthetic powders like ours are very fine-grained (1–10 nm) and contain some structural H_2O while natural magnetites are often micrometer-sized or larger and are usually derived from igneous processes (i.e., little structural water).

Based on the compositional, solubility, and mineralogical data, we can estimate the relative proportions of phases in our MT-RT series samples from the following equations:

$$\text{Magnetite + ferrihydrite} = 1.43(Fe_O) + 1.89(Al_O) \quad (1)$$

$$\text{Goethite} = 1.43(Fe_d - Fe_O) + 1.89(Al_d - Al_O) + H_2O_{Gt} \quad (2)$$

$$\text{Gibbsite} = 1.89(Al_{total} - Al_d) + H_2O_{Gb} \quad (3)$$

These equations assume that the magnetites and the ferrihydrite-like phases are the only oxalate-soluble phases, that gibbsite is not soluble in either extractant, and that Fe and Al are congruently soluble. The TEM and Mössbauer data show that magnetite + ferrihydrite is predominantly magnetite for $Al_s < 0.20$. For the purposes of these approximate calculations, all Fe was taken as ferric iron, negative concentrations were set equal to zero, and H_2O was added in stoichiometric proportions for goethite and gibbsite. The results of the calculations (Figure 10) agree qualitatively with XRD data.

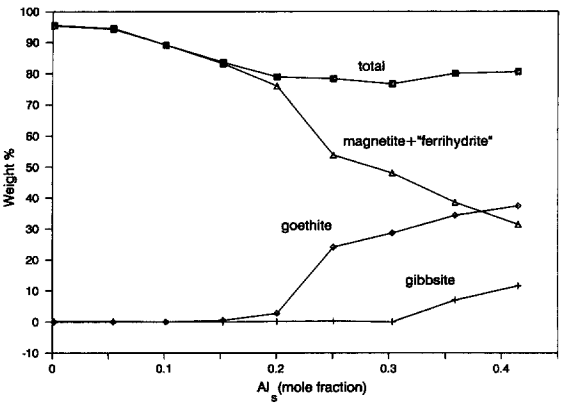

Figure 10. Approximate mineralogical composition of unheated powders (MT-RT series) estimated from solubility data.

The weight total for the oxides does not sum to 100. The deficit is about 5 wt. % for MT-RT-00 and increases to and levels out at 20–25 wt. % by $Al_s = 0.20$. The deficit probably results from adsorbed H_2O and structural H_2O not associated with goethite and gibbsite. The ferrihydrite-like phase observed in the TEM and Mössbauer data of MT-RT-20 but not MT-RT-00 implies that the increase in deficit with increasing Al_s results at least in part from structural H_2O associated with the ferrihydrite-like phase.

The above calculations also imply that the molar ratio $Al_o/(Al_o + Fe_o)$ is a better measure of the degree of Al substitution in the magnetites than is Al_s. As shown in Figure 9, equivalent values are obtained except for the three samples with the highest values of Al_s. These samples contain significant amounts of gibbsite so that the values of Al_s for these three samples overestimates the degree of Al substitution.

MT-400 and MT-500 series samples

Upon heating, the MT-RT powders (mostly cation deficient magnetite for $Al_s < 0.2$) thermally decompose to a mixture of maghemite and hematite at 400°C and then to hematite at 500°C. Although impurity phases (goethite, lepidocrocite, ferrihydrite, and gibbsite) appear for $Al_s > 0.20$, they all transform to hematite by 500°C except gibbsite.

The oxalate solubility for the three series of samples increases in the order MT-RT > MT-400 > MT-500. This could imply mineral solubility in the order magnetite > maghemite > hematite. However, the observed order of solubility could instead result from other changes in properties that would give the observed order in solubility. These include particle size and crystallinity which, as shown by XRD and TEM

data, both change in a way (MT-RT < MT-400 < MT-500) to give the observed order of solubilities. Presence of excess hydroxyls or water in the mineral also may enhance oxalate extractability (Stanjek and Weidler, 1992).

Although Fe and Al are extracted in the same ratio as in the bulk solid phase by oxalate for the MT-RT samples, they are not extracted in the same way for MT-400 and especially for MT-500 samples (Figure 9). For the MT-500 (hematite) samples, the strong positive deviation from the slope = 1.0 line implies that Al goes into oxalate solution in preference to Fe. Possible explanations for this behavior include 1) exsolution of Al from Fe-oxides as they are heated as amorphous, Al-rich $(Al,Fe)_2O_3$ and (Al,Fe)OOH and 2) migration of Al to surface regions of particles as a consequence of heating.

ACKNOWLEDGMENTS

Critical comments by Carlton Allen and two anonymous reviewers are gratefully acknowledged.

REFERENCES

Anand, R. R. and Gilkes, R. J. (1984) Mineralogical and chemical properties of weathered magnetite grains from lateritic saprolite: *J. of Soil Sci.* **35,** 559–567.

Haley, G., Mullen, J. G., and Honig, J. M. (1989) First order change in hyperfine interaction at the Vervey transition in magnetite: *Sol. State Comm.* **69,** 285–287.

Jackson, M. L. (1974) *Soil Chemical Analysis-Advanced Course:* 2nd ed., 9th printing, published by the author, Department of Soil Science, University of Wisconsin, Madison, 895 pp.

Jolivet, J. P., Tronc, B. E., and Livage, J. (1992) Influence of Fe(II) on the formation of the spinel iron oxide in alkaline medium: *Clays & Clay Minerals* **40,** 531–540.

McKeague, J. A. and Day, J. H. (1966) Dithionite and oxalate extractable Fe and Al as aids in differentiating various classes of soils: *Can. J. Soil Sci.* **46,** 13–22.

Morris, R. V., Schulze, D. G., Lauer Jr., H. V., Agresti, D. G., and Shelfer, T. D. (1992) Reflectivity (Visible and Near IR), Mössbauer, static magnetic and X-ray diffraction properties of aluminum-substituted hematites: *J. Geophys. Res.* **97,** 10257–10266.

Morris, R. V. and Lauer, H. V. (1990) Matrix effects for reflectivity spectra of dispersed nanophase (superparamagnetic) hematite with application to Martian spectral data: *J. Geophys. Res.* **95,** 5101–5109.

Morris, R. V., Lauer Jr., H. V., Lawson, C. A., Gibson Jr., E. K., Nace, G. A., and Stewart, C. (1985) Spectral and other physicochemical properties of submicron powders of hematite (α-Fe_2O_3), maghemite (γ-Fe_2O_3), magnetite (Fe_3O_4), goethite (α-FeOOH), and lepidocrocite (γ-FeOOH): *J. Geophys. Res.* **90,** 3126–3144.

Murad, E., Bowen, L. H., Long, G. J., and Quin, T. G. (1988) The influence of crystallinity in magnetic ordering in natural ferrihydrites: *Clay Miner.* **23,** 161–173.

Pawluk, S. (1972) Measurement of crystalline and amorphous iron removal in soil: *Can. J. Soil Sci.* **52,** 119–123.

Rhoton, F. E., Bigham, J. M., Norton, L. D., and Smeck, N. E. (1981) Contribution of magnetite to oxalate-extractable iron in soils and sediments from the Maumee River basin of Ohio: *Soil Sci. Soc. Amer. J.* **45,** 645–649.

Saunders, W. M. H. (1965) Phosphate retention by New Zealand soils and its relationship to free sesquioxides, organic matter, and other soil properties: *New Zealand J. Agr. Res.* **8,** 30–57.

Schwertmann, U. (1964) The differentiation of iron oxides in soils by a photochemical extraction with acid ammonium oxalate: *Z. Pflanzenernahr Dung. Bodenk.* **105,** 194–201.

Schwertmann, U. and Murad, E. (1990) The influence of aluminum on iron oxides: XIV. Al-substituted magnetite synthesized at ambient temperatures. *Clays & Clay Minerals* **38,** 196–202.

Sherman, D. M. and Waite, T. D. (1985) Electronic spectra of Fe^{3+} oxides and oxide hydroxides in the near IR and near UV: *Amer. Mineral.* **70,** 1262–1269.

Sidhu, P. S., Gilkes, R. J., and Posner, A. M. (1981) Oxidation and ejection of nickel and zinc from natural and synthetic magnetite: *Soil Sci. Soc. Amer. J.* **45,** 641–644.

Stanjek, H. and Schwertmann, U. (1992) The influence of aluminum on iron oxides. Part XVI: Hydroxyl and aluminum substitution in synthetic hematites: *Clays & Clay Minerals* **40,** 347–355.

Stanjek, H. and Weidler, P. G. (1992) The effect of dry heating on the chemistry, surface area, and oxalate solubility of synthetic 2-line and 6-line ferrihydrite: *Clays & Clay Minerals* **27,** 397–412.

Stucki, J. W. (1981) The quantitative assay of minerals for Fe^{2+} and Fe^{3+} using 1,10 phenanthroline. II. A photochemical method: *Soil Sci. Soc. Amer. J.* **45,** 638–641.

Weidner, V. R. and Hsia, J. J. (1981) Reflection properties of pressed polytetrafluoroethylene powder: *J. Opt. Soc. Am.* **71,** 856–861.

Zussman, J. (1977) X-ray diffraction: in *Physical Methods in Determinative Mineralogy,* J. Zussman, ed., Academic Press, New York, 391–471.

(Received 10 June 1993; accepted 7 October 1993; Ms. 2385)